Liquid Crystals
Publication details, including instructions for authors and subscription information:
http://www.informaworld.com/smpp/title~content=t713926090

The effect of mesogenic and non-mesogenic crosslinking units on the phase behaviour of side-chain smectic and cholesteric elastomers

Jian-She Hu[a]; Li-Qun Yang[a]; Dan-Shu Yao[a]; Zhi-Wei Song[a]
[a] Center for Molecular Science and Engineering, College of Science, Northeastern University, Shenyang, People's Republic of China

Online publication date: 15 November 2010

To cite this Article Hu, Jian-She , Yang, Li-Qun , Yao, Dan-Shu and Song, Zhi-Wei(2010) 'The effect of mesogenic and non-mesogenic crosslinking units on the phase behaviour of side-chain smectic and cholesteric elastomers', Liquid Crystals, 37: 11, 1385 — 1392
To link to this Article: DOI: 10.1080/02678292.2010.517327
URL: http://dx.doi.org/10.1080/02678292.2010.517327

Liquid Crystals,
Vol. 37, No. 11, November 2010, 1385–1392

Taylor & Francis
Taylor & Francis Group

The effect of mesogenic and non-mesogenic crosslinking units on the phase behaviour of side-chain smectic and cholesteric elastomers

Jian-She Hu*, Li-Qun Yang, Dan-Shu Yao and Zhi-Wei Song

Center for Molecular Science and Engineering, College of Science, Northeastern University, Shenyang, People's Republic of China

(*Received 2 August 2010; final version received 17 August 2010*)

Chiral monomer ($\mathbf{M_1}$), mesogenic and non-mesogenic crosslinking agents ($\mathbf{C_1}$ and $\mathbf{C_2}$), and the corresponding liquid crystalline elastomers ($\mathbf{P_1}$ and $\mathbf{P_2}$ series), have been synthesised. Their chemical structures have been characterised by Fourier transform infrared or ^{1}H nuclear magnetic resonance and their phase behaviour investigated by differential scanning calorimetry, polarising optical miscoscopy, thermo-gravimetric analysis (TGA) and X-ray diffraction. The effect of the crosslinking unit on the phase behaviour of the elastomers has been studied. $\mathbf{M_1}$ showed a cholesteric oily streak and focal conic texture. $\mathbf{C_2}$ exhibited a nematic enantiotropic thread-like and schlieren texture, and a monotropic fan-shaped texture in the S_A phase. Due to the introduction of the mesogenic crosslinking unit, elastomers, $\mathbf{P_{2\text{-}1}}-\mathbf{P_{2\text{-}5}}$, exhibited a cholesteric phase, while elastomers, $\mathbf{P_{1\text{-}1}}-\mathbf{P_{1\text{-}4}}$, derived from a non-mesogenic crosslinking unit, exhibit a S_A phase. As the content of the crosslinking unit increased, the T_g of the $\mathbf{P_1}$ series initially decreased and then increased, and the T_i of the series decreased. In the $\mathbf{P_2}$ series the T_g increased, but the T_i initially increased and then decreased. TGA confirmed that all the elastomers had improved thermal stability.

Keywords: liquid crystalline elastomers; phase behaviour; mesogenic crosslinking unit; smectic phase; cholesteric phase

1. Introduction

Liquid crystalline elastomers (LCEs) have attracted considerable attention in recent years due to a unique combination of the rubber elasticity of polymer networks and the anisotropic optical and electrical characteristics of conventional liquid crystalline (LC) phases [1–17]. LCEs exhibit complex mechanical behaviour, arising from the coupling of the orientational degrees of freedom of the mesogenic order with those of the rubber elastic matrix. Consequently, LCEs show not only entropic elasticity but also reversible LC phase transitions.

Among the various mesophases, nematic LCEs have so far received the most attention, whereas smectic or cholesteric LCEs are, at least from the theoretical standpoint, considerably less well understood. Smectic LCEs are composed of mesogenic polymers, which make up the layered smectic phase, so these LCEs exhibit distinct anisotropic mechanical properties and mechanical deformation processes parallel to or perpendicular to the normal of the smectic layer, causing different responses of the networks [18–23]. The piezoelectricity of cholesteric LCEs, arising from the physical effects of polarisation induced by mechanical deformation, has been unquestioned [24]. Cholesteric LCEs have the potential to be able to transform a mechanical signal into an electric signal when stress is applied parallel to the cholesteric helix. They are therefore candidates for use in piezoelectric devices.

A number of smectic [18–23] or cholesteric [24–33] LCEs have been previously prepared, mainly involving the use of mesogenic monomers and bifunctional non-mesogenic crosslinking agents. To the best of our knowledge, however, in the cholesteric LCEs already reported, especially those employing polysiloxane as backbone, mesogenic crosslinking agents have rarely been involved.

The objectives of the present research were, firstly, to study the effect of mesogenic and non-mesogenic crosslinking units on the mesomorphism and phase behaviour of LCEs, and secondly, to produce cholesteric elastomers based on a mesogenic crosslinking unit. Two series of novel smectic and cholesteric LCEs have been prepared by reacting a chiral LC monomer with mesogenic or non-mesogenic crosslinking agents. Their phase behaviour has been characterised by differential scanning calorimetry (DSC), polarising optical microscopy (POM), X-ray diffraction (XRD) and thermo-gravimetric analysis (TGA). The effect of the mesogenic and non-mesogenic crosslinking units on the phase behaviour of the elastomers has been established.

*Corresponding author. Email: hujs@mail.neu.edu.cn

ISSN 0267-8292 print/ISSN 1366-5855 online

DOI: 10.1080/02678292.2010.517327
http://www.informaworld.com

2. Experimental

2.1 Materials

Hexanedioic acid was purchased from Shenyang Xinxi Reagent Co. (Shenyang, China), and cholesterol from Henan Xiayi Medical Co. (Xiayi, China). 4-Hydroxybenzoic acid was obtained from Shanghai Wulian Chemical Plant (Shanghai, China), and allyl bromide from Beijing Chemical Reagent Co. (Beijing, China). Undecylenic acid was purchased from Beijing Jinlong Chemical Reagent Co. Ltd. (Beijing, China), and polymethylhydrosiloxane (PMHS, $\overline{M}_n = 700 - 800$) from Jilin Chemical Industry Co. (Jilin, China). The toluene used in the hydrosilylation reaction was purified by treatment with lithium aluminium hydride and distilled prior to use. All other solvents and reagents used were purified using standard methods.

2.2 Measurements

FT-IR spectra were measured on a Perkin–Elmer Spectrum One (B) spectrometer (Perkin–Elmer, Foster City, CA), and ^{1}H NMR spectra were obtained using a Bruker ARX300 spectrometer (Bruker, Switzerland). Thermal properties were determined using a Netzsch DSC 204 (Netzsch, Hanau, Germany) equipped with a cooling system, at heating and cooling rates of 10°C min^{-1}. The thermal stability of the polymers was measured under nitrogen with a Netzsch TGA 209C thermo-gravimetric analyser, using a heating rate of 20°C min^{-1}. A Leica DMRX polarising optical microscope (Leica, Germany), equipped with a Linkam THMSE–600 (Linkam, Tadworth, Surrey, UK) cool and hot stage, was employed to observe the optical textures and phase transition temperatures. XRD measurements were performed under nickel-filtered Cu–K_α radiation using a DMAX–3A Rigaku (Rigaku, Japan) powder diffractometer.

2.3 Synthesis of the chiral monomer

The synthetic route for the chiral monomer is outlined in Scheme 1. 4-Allyloxybenzoic acid (**1**) and 4-hydroxyphenyl-4′-allyloxybenzoate (**3**) were prepared using methods reported previously [34].

2.3.1 6-Cholesteryloxy-6-oxohexanoic acid (5)

Hexanedioic acid (73.0 g, 0.5 mol) and 120 mL of thionyl chloride, together with a few drops of dimethylformamide (DMF), were reacted for 2 h at room temperature and 5 h at 60°C. The excess thionyl chloride was removed under reduced pressure to yield the acid chloride, **4**. A solution of cholesterol (38.7 g, 0.1 mol) in 100 mL chloroform and 8 mL pyridine was added drop-wise under rapid stirring to a solution of **4** in 200 mL chloroform. The mixture was allowed to react at room temperature for 2 h and then refluxed

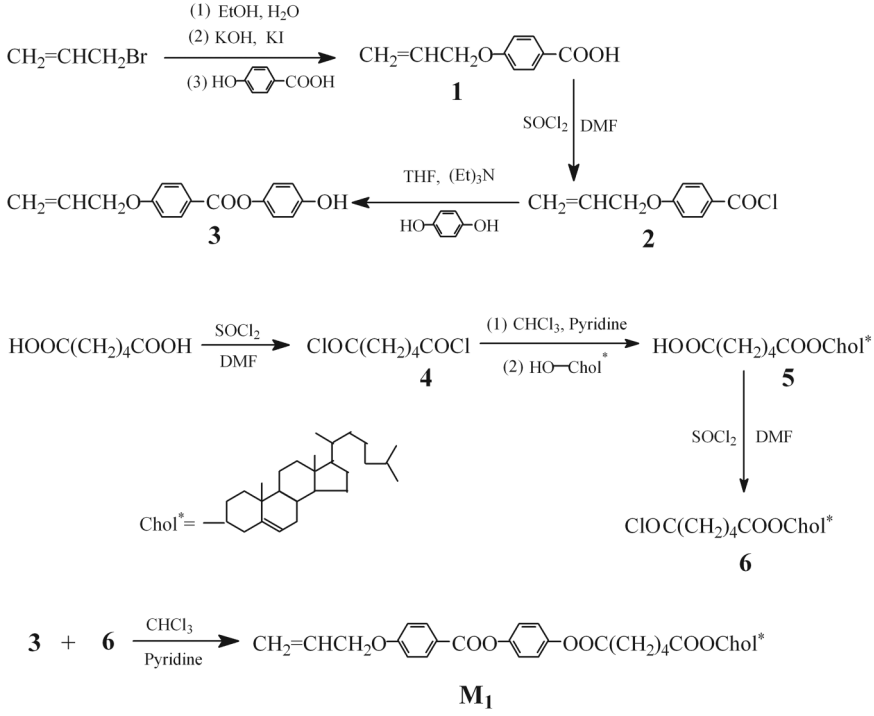

Scheme 1. Synthetic route to the chiral monomer, $\mathbf{M_1}$.

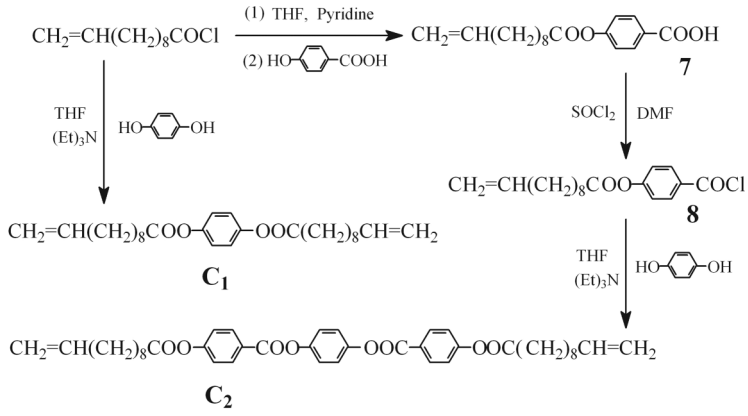

Scheme 2. Synthetic route to the crosslinking agents, $\mathbf{C_1}$ and $\mathbf{C_2}$.

for 15 h. After removing the solvent on a rotary evaporator, the solid residue was poured into 1000 mL ice-water and stirred for 1 h. The crude product was then filtered off and washed a number of times with warm water and ethanol, and then recrystallised from acetone (yield 67%):

$[\alpha]_D^{20}$ –29.6° ($CHCl_3$), phase transition: K 137.0 (76.8) Ch 148.3 (4.0) I.
IR (KBr): 3250–2540 (–COOH); 2956, 2819 (CH_3–, $–CH_2–$); 1738, 1680 cm^{-1} (C=O).
^{1}H NMR ($CDCl_3$, TMS, δ): 0.75–2.61 [m, 51H, $–(CH_2)_4–$ and cholesteryl –***H***]; 4.60 (m, 1H, –C***H***< in cholesteryl); 5.36 (d, 1H, >C=C***H***– in cholesteryl); 11.56 (s, 1H, –COO***H***).

*2.3.2 4-(4-(Allyloxy)benzoyloxy)phenyl cholesteryl adipate (**M$_1$**)*

Compound **6** (5.33 g, 0.01 mol), dissolved in 10 mL of chloroform, was added drop-wise under stirring to a solution of compound **3** (2.72 g, 0.01 mol) in 20 mL chloroform and 0.8 mL pyridine. The mixture was refluxed for 36 h, cooled to room temperature and filtered. The filtrate was concentrated and the crude product precipitated by adding methanol, filtered off and recrystallised from chloroform : methanol (1 : 2) (yield 54%):

$[\alpha]_D^{22}$ –22.8° ($CHCl_3$).
IR (KBr): 3075 (=C–H); 2948, 2867 (CH_3–, $–CH_2–$); 1761, 1731 (C=O); 1649 (C=C); 1606–1510 (Ar–); 1253 cm^{-1} (C–O–C).
^{1}H NMR ($CDCl_3$, TMS, δ): 0.70–2.62 [m, 51H, $–(CH_2)_4–$ and cholesteryl –***H***]; 4.65 (m, 3H, $–CH_2O–$ and –C***H***< in cholesteryl); 5.34–5.50 (m, 3H, $CH_2=$ and >C=C***H***– in cholesteryl); 6.05–6.14 (m, 1H, $CH_2=CH–$); 7.01–8.18 (m, 8H, Ar–***H***).

2.4 Synthesis of the crosslinking agent

The synthetic route for the crosslinking agent is outlined in Scheme 2. $\mathbf{C_1}$ and $\mathbf{C_2}$ were prepared according to the methods reported previously [35].

*2.4.1 Phenyl 4,4′-bis(undec-10-enoate) (**C$_1$**)*

After recrystallisation from ethanol, white crystals were obtained (yield 62%):

IR (KBr): 3075 (=C–H); 2923, 2851 (CH_3–, $–CH_2–$); 1746 (C=O); 1641 (C=C); 1504–1469 cm^{-1} (Ar–).
^{1}H NMR ($CDCl_3$, TMS, δ): 1.29–1.83 [m, 24H, $–(CH_2)_6–$]; 2.02–2.08 (m, 4H, $CH_2=CH–CH_2–$); 2.56–2.62 (t, 4H, $–CH_2COO–$); 4.97–5.05 (m, 4H, $CH_2=CH–$); 5.77–5.84 (m, 2H, $CH_2=CH–$); 7.06 (m, 4H, Ar–***H***).

*2.4.2 Phenyl 4,4′-bis(4-(undec-10-enoyloxy) benzoate) (**C$_2$**)*

After recrystallisation from ethanol, white crystals were obtained (yield 66%):

IR (KBr): 3073 (=C–H); 2926, 2854 (CH_3–, $–CH_2–$); 1758, 1734 (C=O); 1640 (C=C); 1603–1508 cm^{-1} (Ar–).
^{1}H NMR ($CDCl_3$, TMS, δ): 1.27–1.82 [m, 24H, $–(CH_2)_6–$]; 2.03–2.10 (m, 4H, $CH_2=CH–CH_2–$); 2.58–2.63 (t, 4H, $–CH_2COO–$); 4.95–5.05 (m, 4H, $CH_2=CH–$); 5.79–5.85 (m, 2H, $CH_2=CH–$); 7.21–8.18 (m, 12H, Ar–***H***).

2.5 Synthesis of the elastomers

The elastomers, $\mathbf{P_1}$ and $\mathbf{P_2}$ series, were synthesised by similar methods, and their polymerisation feed ratio and yields are summarised in Table 1.

Table 1. Polymerisation and yields.

P_1 series	C_1[a] (mol%)	Yield (%)	P_2 series	C_2[b] (mol%)	Yield (%)
$P_{1\text{-}0}$	0	92	$P_{2\text{-}0}$	0	92
$P_{1\text{-}1}$	2	95	$P_{2\text{-}1}$	2	93
$P_{1\text{-}2}$	4	93	$P_{2\text{-}2}$	4	92
$P_{1\text{-}3}$	8	94	$P_{2\text{-}3}$	8	94
$P_{1\text{-}4}$	12	93	$P_{2\text{-}4}$	12	91
$P_{1\text{-}5}$	15	95	$P_{2\text{-}5}$	15	93

Notes: [a]Molar fraction of C_1 based on ($M_1 + 2C_1$).
[b]Molar fraction of C_2 based on ($M_1 + 2C_2$).

As an example, the synthesis of $P_{1\text{-}3}$ was as follows. M_1, C_1 and PMHS were dissolved in dry toluene. The reaction mixture was heated to 65°C under nitrogen, and 2 ml of a solution of H_2PtCl_6 catalyst (5 mg ml^{-1}) in THF was injected into mixture using a syringe. The progress of the hydrosilylation reaction, monitored by the Si−H stretch intensity, proceeded to completion, and this was confirmed by infrared (IR) measurements. $P_{1\text{-}1}$ was obtained by pouring the toluene solution into methanol; the precipitate was washed with hot ethanol and dried *in vacuo*.

3. Results and discussion

3.1 Synthesis

The chemical structures of the target monomer and crosslinking agents were characterised by Fourier transform infrared (FT–IR) and ^{1}H nuclear magnetic resonance (NMR) and were in agreement with those predicted. The IR spectra of M_1 showed characteristic stretching bands around 1761 cm^{-1}, attributed to ester C=O linked to a cholesteryl group, and at 1731 cm^{-1} due to ester C=O linked to an aromatic ring. IR spectra of C_2 showed characteristic stretching bands around 1758 cm^{-1} attributed to ester C=O in undecylenate, and at 1734 cm^{-1} attributed to ester C=O in substituted benzoate. The ^{1}H NMR spectra of M_1 showed a multiplet at 6.14–5.34 ppm, corresponding to olefinic protons in the allyl group. Both C_1 and C_2 showed a multiplet at 5.85–4.95 ppm, corresponding to olefinic protons in undecylenate. As an example, the ^{1}H NMR spectra of M_1 are shown in Figure 1.

The elastomers, P_1 and P_2 series, were prepared by hydrosilylation. The elastomers obtained were insoluble in solvents such as toluene or chloroform. The IR spectra of these elastomers showed complete disappearance of the Si–H stretching band in PMHS at about 2168 cm^{-1} and the olefinic C=C stretching band at 1649–1640 cm^{-1}. Characteristic Si–C bands appeared at about 1268 and 778 cm^{-1}, and Si–O–Si bands were present at 1168, 1129 and 1029 cm^{-1} in $P_{1\text{-}3}$.

3.2 Phase behaviour of the monomer and crosslinking agent

The phase behaviour of the target monomer and crosslinking agent were investigated using DSC and POM. The phase transition temperatures, corresponding enthalpy changes and mesophase types are summarised in Table 2.

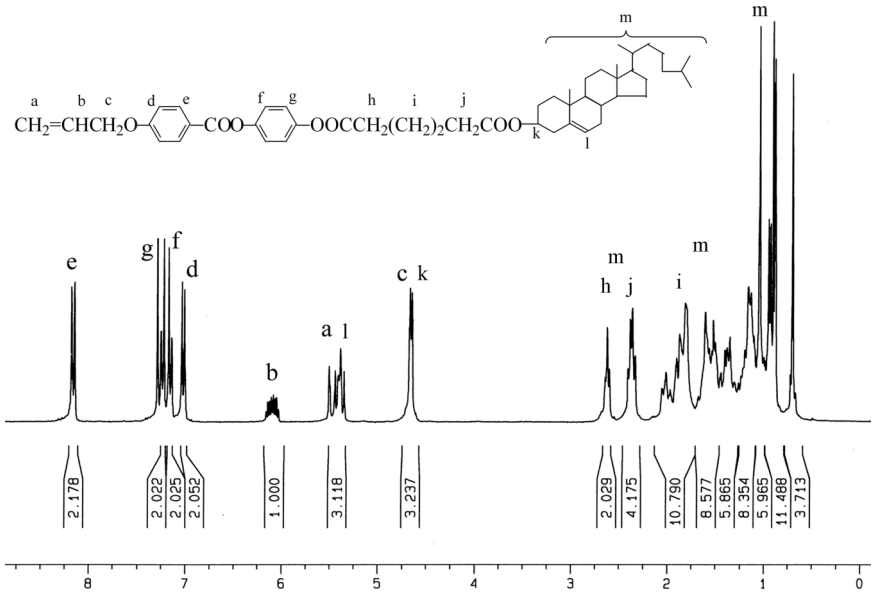

Figure 1. ^{1}H NMR spectrum of M_1.

Table 2. Thermal properties of monomer and crosslinking agents.

Sample	Mesophase and phase transition temperature (°C), and enthalpy changes (J g^{-1})	
	Heating cycle	Cooling cycle
M_1	Cr 132.8(42.9) Ch193.0(14.6)I	I180.0(8.6) Ch–Cr
C_1	Cr 70.6 (189.2)I	I61.5(188.1) Cr
C_2	Cr 116.4(15.3) N170.5(1.8)I	I167.8(1.6)N120.8(0.8) S_A101.2(9.3) Cr

Notes: Cr = crystal; Ch = cholesteric phase; N = nematic; S_A = smectic A; I = isotropic phase.

DSC heating curves of **M_1** and **C_2** showed a melting transition and a transition from LC to the isotropic phase, respectively. On cooling, only an isotropic to cholesteric phase transition was seen in **M_1**, and a crystallisation transition did not appear, due to supercooling occurring in the samples; three exothermic peaks were seen for **C_2**, which represent an isotropic to nematic phase transition, a nematic to smectic A (S_A) phase transition, and a S_A to crystallisation transition, respectively. However, DSC curves of **C_1** showed only a melting transition and crystallisation transition on heating and cooling.

The POM results showed that **M_1** exhibited enantiotropic oily streak texture during the heating cycle and focal conic texture of the cholesteric phase during cooling. Moreover, the focal conic texture was readily transformed to oily steak texture by shearing the mesophase. Optical micrographs of **M_1** are illustrated in Figure 2.

C_1 did not show mesomorphism, but **C_2** exhibited enantiotropic nematic thread-like texture and schlieren texture, and monotropic fan-shaped texture of the S_A phase. Optical micrographs of **C_2** are shown in Figure 3.

3.3 Phase behaviour of the elastomers

The phase behaviour and thermal stability of the elastomers were investigated using DSC, POM, TGA and XRD. The corresponding phase transition temperatures and thermal decomposition temperatures are summarised in Tables 3 and 4.

DSC thermograms of the elastomers **$P_{1\text{-}1}$**–**$P_{1\text{-}4}$** and **$P_{2\text{-}1}$**–**$P_{2\text{-}4}$** showed a glass transition and phase

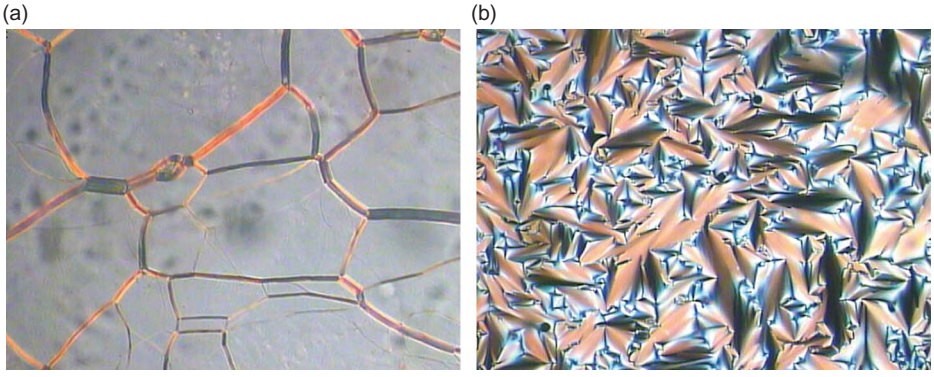

Figure 2. Optical textures of monomer, **M_1** (200×): (a) oily streak texture of cholesteric phase on heating to 145.3°C; (b) focal conic texture of cholesteric phase on cooling to 148.3°C (colour version online).

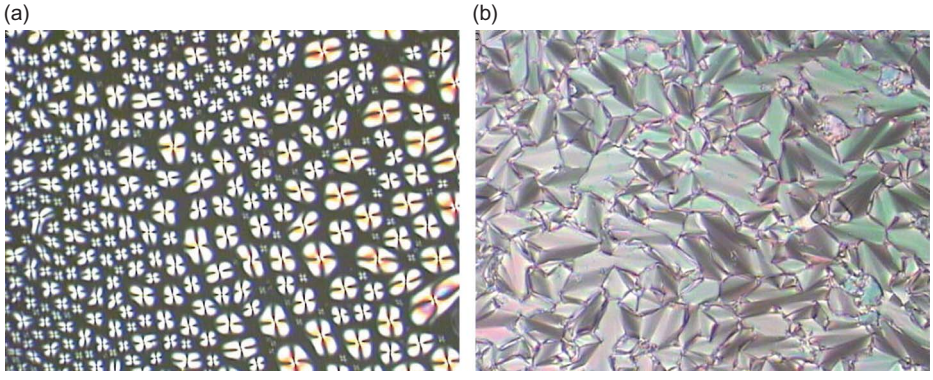

Figure 3. Optical textures of crosslinking agent, **C_2** (200×): (a) droplet texture with schlieren of nematic phase on cooling to 163.5°C; (b) fan-shaped texture of smectic A phase on cooling to 120.6°C (colour version online).

Table 3. Thermal properties of elastomers, **P$_1$** series.

P$_1$ series	T_g (°C)	T_i (°C)	ΔT[b]	T_d[c] (°C)
P$_{1\text{-}0}$	50.3	223.5	173.2	294.0
P$_{1\text{-}1}$	45.6	217.7	172.1	301.5
P$_{1\text{-}2}$	35.8	201.5	165.7	307.8
P$_{1\text{-}3}$	36.7	196.2	159.5	309.6
P$_{1\text{-}4}$	41.5	190.6[a]	149.1	313.2
P$_{1\text{-}5}$	47.3	–	–	316.7

Notes: [a]Temperature observed with POM.
[b]Mesophase temperature range (T_i–T_g).
[c]Temperature by which 5% weight loss had occurred.

Table 4. Thermal properties of elastomers, **P$_2$** series.

P$_2$ series	T_g (°C)	T_i (°C)	ΔT[b]	T_d[c] (°C)
P$_{2\text{-}0}$	50.3	223.5	173.2	294.0
P$_{2\text{-}1}$	47.4	238.3	190.9	303.7
P$_{2\text{-}2}$	48.6	240.5	191.9	305.3
P$_{2\text{-}3}$	50.9	236.6	185.7	312.5
P$_{2\text{-}4}$	54.2	232.7	178.5	311.8
P$_{2\text{-}5}$	56.5	231.5[a]	175.0	315.9

Notes: [a]Temperature observed with POM.
[b]Mesophase temperature range (T_i–T_g).
[c]Temperature by which 5% weight loss occurred.

transition from LC to isotropic. Moreover, the POM results showed that all the elastomers apart from **P$_{1\text{-}5}$** exhibited mesomorphism. This indicates that low levels of chemical crosslinking do not significantly affect the phase behaviour of the elastomers, and reversible mesophase transitions can be observed as a result of sufficient mesogenic molecular motion. On the other hand, high levels of crosslinking have a strong influence on phase behaviour and can cause the mesophase to disappear, due to the disturbance and depression of mesogenic orientational order. For this reason the DSC curve of **P$_{1\text{-}5}$** showed only glass transition. TGA results showed that the temperature at which 5% weight loss occurred (T_d) was above 300°C for all the elastomers, confirming their high thermal stability.

The glass transition temperature (T_g) is an important parameter in regard to both structures and properties. In general chemical crosslinking imposes additional constraints on the motion of chain segments, causing a reduction in free volume and an increase in T_g. However, the effect may be small for lightly crosslinked polymers containing a flexible crosslinking unit with long spacer, and T_g is also affected by the flexible crosslinking chains, similar to a plasticising effect. Compared with homopolymers, T_g of lightly crosslinked polymers may fall. Taking the crosslinking effect and plasticising effect into account, T_g is given by

$$T_g = T_{go} - K_x \rho_x, \quad (1)$$

$$T_g = T_{go} + K_x \rho_x, \quad (2)$$

where T_g and T_{go} are the glass transition temperatures of crosslinked and non-crosslinked polymers, respectively, K_x is a constant, and ρ_x is the crosslinking density. When the crosslinking density is below a certain critical value, the plasticising effect of the flexible crosslinking chains predominates, and Equation (1) applies. Conversely, when the crosslinking effect is predominant, Equation (2) becomes applicable.

According to Table 3, T_g decreased from 50.3°C for **P$_{1\text{-}0}$** to 35.8°C for **P$_{1\text{-}2}$**. However, there was a general tendency towards an increase in T_g with increasing content of the **C$_1$** crosslinking unit. T_g increased from 35.8°C for **P$_{1\text{-}2}$** to 47.3°C for **P$_{1\text{-}5}$** when the content of the **C$_1$** crosslinking unit increased from 4 to 15 mol%. Similarly to the **P$_1$** series, as the content of **C$_2$** crosslinking unit increased from 2 to 15 mol%, the T_g of the **P$_2$** series increased from 47.4°C for **P$_{2\text{-}1}$** to 56.5°C for **P$_{2\text{-}5}$**.

In addition, chemical crosslinking was also seen to affect the isotropic temperature (T_i) of the mesophase. In general, a non-mesogenic crosslinking unit acts as diluent and caused a decrease in T_i. According to Table 3, T_i decreased from 223.5°C for **P$_{1\text{-}0}$** to 190.6°C for **P$_{1\text{-}4}$** as the content of **C$_1$** crosslinking unit increased from 0 to 12 mol%. However, the LC properties of the mesogenic crosslinking unit may cause an increase in T_i. For the **P$_2$** series, based on a mesogenic crosslinking unit, the corresponding T_i increased from 223.5 for **P$_{2\text{-}0}$** to 240.5°C for **P$_{2\text{-}2}$**. However, higher crosslinking density can prevent the motion and orientation of mesogenic molecules in the vicinity of the crosslinking sites, and it does not favour the formation of mesogenic orientational order in the networks. T_i was therefore found to disappear when the crosslinking density was greater than the critical value. In the **P$_1$** series, the mesophase disappeared when the content of the **C$_1$** crosslinking unit was greater than 12 mol%. However, only stress-induced birefringence of the elastomer **P$_{2\text{-}5}$** could be observed, even though the content of the **C$_2$** crosslinking unit was 15 mol%.

The polymers **P$_{1\text{-}0}$** and **P$_{2\text{-}0}$** and elastomers **P$_{1\text{-}1}$**–**P$_{1\text{-}4}$** exhibited a batonnet texture in the S_A phase, although their corresponding monomers showed a cholesteric phase. However, the elastomers **P$_{2\text{-}1}$**–**P$_{2\text{-}5}$** exhibited Grandjean texture in the cholesteric phase following the introduction of the nematic crosslinking unit.

In order to obtain a more detailed mesophase type, XRD studies were carried out. In general, a sharp peak associated with the smectic layers at a small

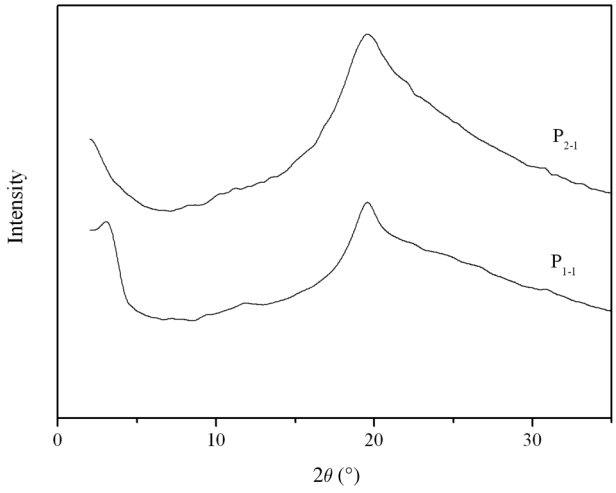

Figure 4. XRD curves of $\mathbf{P_{1\text{-}1}}$ and $\mathbf{P_{2\text{-}1}}$ at mesophase.

angle ($2\theta < 5°$), and a broad peak associated with the lateral packings at a wide angle, could be observed for the smectic phase structure. For $\mathbf{P_{1\text{-}0}}$–$\mathbf{P_{1\text{-}4}}$ and $\mathbf{P_{2\text{-}0}}$, the X-ray patterns exhibited a sharp reflection at $2\theta \approx 3.0°$; the *d*-spacing of the first-order reflections was about 29.5Å, and a broad peak occurred at $2\theta \approx 20°$. Moreover, the *d*-spacing of the first-order reflection hardly changed with temperature. This gives strong evidence for the formation of the S_A phase. In the case of $\mathbf{P_{2\text{-}1}}$–$\mathbf{P_{2\text{-}5}}$, no peak appeared in the small-angle X-ray scattering curve, but a broad peak occurred at $2\theta \approx 20°$. As an example, Figure 4 shows the XRD curves for $\mathbf{P_{1\text{-}1}}$ and $\mathbf{P_{2\text{-}1}}$ at the mesophase. The smectic structure of $\mathbf{P_{1\text{-}0}}$–$\mathbf{P_{1\text{-}4}}$ and $\mathbf{P_{2\text{-}0}}$ and the cholesteric structure of $\mathbf{P_{2\text{-}1}}$–$\mathbf{P_{2\text{-}5}}$ were thus confirmed by the POM and XRD results.

4. Conclusions

A new cholesteric monomer, $\mathbf{M_1}$, a non-mesogenic crosslinking agent, $\mathbf{C_1}$, a mesogenic crosslinking agent, $\mathbf{C_2}$, and corresponding elastomers based on a polysiloxane backbone have been synthesised and characterised. $\mathbf{M_1}$ showed a cholesteric phase. $\mathbf{C_1}$ showed no LC texture, and $\mathbf{C_2}$ revealed an enantiotropic nematic phase and a monotropic S_A phase. The elastomers $\mathbf{P_{1\text{-}1}}$–$\mathbf{P_{1\text{-}4}}$, based on a non-mesogenic crosslinking agent, exhibited a batonnet texture in the S_A phase. However, the elastomers $\mathbf{P_{2\text{-}1}}$–$\mathbf{P_{2\text{-}5}}$ exhibited cholesteric Grandjean texture due to the introduction of the nematic crosslinking unit. The elastomers containing less than 15 mol% of crosslinking units displayed elasticity and reversible mesophase transition. In the $\mathbf{P_1}$ series, with increasing content of $\mathbf{C_1}$ crosslinking unit, the corresponding T_g first showed a decrease and then an increase, but T_i showed a decrease. In the $\mathbf{P_2}$ series, with increasing content of $\mathbf{C_2}$ crosslinking unit, T_g increased, whereas T_i first showed an increase and then a decrease.

All the elastomers synthesised had good thermal stability.

Acknowledgements

The authors are grateful to the National Science Foundation of China (No. 50503005) and Fundamental Research Funds for the Central Universities (No. N090505002 and N090105001) for financial support during this study.

References

[1] Finkelmann, H.; Kock, H.J.; Rehage, G. *Makromol. Rapid Commun*. **1981**, *2*, 317–322.
[2] Zentel, R.; Reckert, G. *Makromol. Chem*. **1986**, *87*, 1915–1921.
[3] Vallerien, S.U.; Kremer, F. *Makromol. Rapid Commun*. **1990**, *11*, 593–599.
[4] Hikmet, R.A.M.; Lub, J. *Macromolecules* **1992**, *25*, 4194–4201.
[5] Jahromi, S.; Lub, J.; Mol, G.N. *Polymer* **1994**, *35*, 622–629.
[6] Zentel, R.; Brehmer, M. *Liq. Cryst*. **1996**, *6*, 589–596.
[7] Ortiz, C.; Ober, C.K.; Kramer, E.J. *Polymer* **1998**, *39*, 3713–3718.
[8] Hsu, C.S.; Chen, H.L. *J. Polym. Sci., Part A: Polym. Chem*. **1999**, *37*, 3929–3935.
[9] Hirschmann, H.; Roberts, P.M.S.; Davis, F.J.; Guo, W.; Hasson, C.D.; Mitchell, G.R. *Polymer* **2001**, *42*, 7063–7071.
[10] Hiraoka, K.; Uematsu, Y.; Stein, P.; Finkelmann, H. *Macromol. Chem. Phys*. **2002**, *203*, 2205–2210.
[11] Li, M.; Hu, Z.J.; Chen, G.; Chen, X.F. *J. Appl. Polym. Sci*. **2003**, *88*, 2275–2279.
[12] Arai, Y.O.; Urayama, K.; Kohjiya, S. *Polymer* **2004**, *45*, 5127–5135.
[13] Wang, T.L.; Tsai, J.S.; Tseng, C.G. *J. Appl. Polym. Sci*. **2005**, *96*, 336–344.
[14] Saikrasun, S.; Bualek-Limcharoen, S.; Kohjiya, S.; Urayama, K. *J. Polym. Sci., Part B: Polym. Phys*. **2005**, *43*, 135–144.
[15] Rogez, D.; Brandt, H.; Finkelmann, H.; Martinoty, P. *Macromol. Chem. Phys*. **2006**, *207*, 735–745.
[16] Beyer, P.; Terentjev, E.M.; Zentel, R. *Makromol. Rapid Commun*. **2007**, *28*, 1485–1490.
[17] Ren, W.; Mcmullan, P.J.; Griffin, A.C. *Macromol. Chem. Phys*. **2008**, *209*, 1896–1899.
[18] Nishikawa, E.; Finkelmann, H.; Brand, H.R. *Makromol. Rapid Commun*. **1997**, *18*, 65–71.
[19] Aßfalg, N.; Finkelmann, H. *Macromol. Chem. Phys*. **2001**, *202*, 794–800.
[20] Stannarius, R.; Köhler, R.; Dietrich, U.; Lösche, M.; Tolksdorf, C.; Zentel, R. *Phys. Rev. E* **2002**, *65*, 041707 (1)–041707 (11).
[21] Stenull, O. *Phys. Rev. E* **2007**, *75*, 051702 (1)–051702 (10).
[22] Stenull, O.; Lubensky, T.C.; Adams, J.M.; Warner, M. *Phys. Rev. E* **2008**, *78*, 021705 (1)–021705 (7).
[23] Sánchez-Ferrer, A.; Finkelmann, H. *Macromolecules* **2008**, *41*, 970–980.

[24] Pelcovits, R.A.; Meyer, R.B. *J. Phys. II* **1995**, *5*, 877–882.
[25] Broer, D.J.; Lub, J.; Mol, G.N. *Nature* **1995**, *378*, 467–469.
[26] Sapich, B.; Stumpe, J.; Kricheldorf, H.R. *Macromolecules* **1998**, *31*, 1016–1023.
[27] Terentjev, E.M.; Warner, M. *Eur. Phys. J. B* **1999**, *8*, 595–601.
[28] Finkelmann, H. *Adv. Mater*. **2001**, *13*, 1069–1072.
[29] Bermel, P.A.; Warner, M. *Phys. Rev. E* **2002**, *65*, 056614 (1)–056614 (16).
[30] Schmidtke, J.; Stille, W.; Finkelmann, H. *Phys. Rev. Lett*. **2003**, *90*, 083902 (1)-083902 (4).
[31] Menzel, A.M.; Brand, H.R. *Phys. Rev. E* **2007**, *75*, 011707 (1)–011707 (18).
[32] Xing, X.J.; Baskaran, A. *Phys. Rev. E* **2008**, *78*, 021709 (1)–021709 (7).
[33] Hu, J.S.; Zhang, B.Y.; Feng, Z.L.; Wang, H.G.; Zhou, A.J. *J. Appl. Polym. Sci*. **2001**, *80*, 2335–2340.
[34] Hu, J.S.; Zhang, B.Y.; Zhou, A.J.; Yang, L.Q.; Wang, B. *Eur. Polym. J* **2006**, *42*, 2849–2858.